Gyrotron FU series — current status of development and applications

Gyrotron FU series — current status of development and applications

T. Idehara[a,*], S. Mitsudo[a], S. Sabchevski[a], M. Glyavin[a], I. Ogawa[b]

[a]*Research Center for Development of Far-Infrared Region, Fukui University, Fukui 910-8507, Japan*
[b]*Cryogenic Laboratory, Faculty of Engineering, Fukui University, Fukui 910-8507, Japan*

Abstract

The gyrotrons developed at Fukui University ("Gyrotron FU series") are high-frequency, medium-power devices, covering broad frequency bands in the millimeter and submillimeter wavelength regions. Currently, the "Gyrotron FU series" consists of eight gyrotrons. Distinguishing features of these devices are described: Frequency tunability from 38 to 889 GHz; frequency and amplitude modulation of generated radiation; complete cw operation for long periods, exceeding 15 h and high level of stabilization of the output power by feed-back control of the anode potential. The gyrotrons from FU series were successfully used in plasma scattering experiments, electron spin resonance spectroscopy and in-depth studies of mode competition and mode cooperation. In this paper, we summarize and illustrate the achievements of the "Gyrotron FU series" and present some of the ongoing projects for development of novel gyro-devices and quasi-optical transmission systems.

Keywords: Gyrotron; Millimeter-to-submillimeter wavelength region; Frequency modulation; Amplitude modulation; Plasma scattering measurements; ESR spectroscopy; Quasi-optical gyrotron

1. Introduction

The development of gyrotrons is proceeding in two directions. One is the development of high power, millimeter wavelength gyrotrons as power sources for electron–cyclotron heating of plasma, electron–cyclotron current drive of tokamaks as well as for industrial technologies such as ceramic sintering. The second direction is the development of high-frequency, medium-power gyrotrons used, for example, as millimeter-to-submillimeter wavelength sources for plasma scattering measurements and electron spin resonance (ESR) experiments.

The gyrotrons developed at Fukui University (the so-called "Gyrotron FU series") belong to the second group. In recent years, several new high frequency, medium-power gyrotrons covering broad frequency bands in the millimeter and submillimeter wavelength regions have been developed. Currently, the "Gyrotron FU series" consists of eight devices. They have demonstrated many remarkable achievements including frequency tunability from 38 to 889 GHz, high harmonic operation up to fourth harmonics, high-purity mode operation, frequency and amplitude modulations, frequency step switching, complete

cw operation for a long time (more than 15 h), high stabilization of the amplitude by feed-back control of the anode voltage of the electron gun. In-depth studies on the mechanism of the harmonic operation of submillimeter wavelength gyrotrons including investigation of mode competition and mode cooperation have also been performed using these devices. As a result, they have achieved high and stable operational performance.

The research in the field of development and application of gyrotrons is being pursued in close cooperation with the University of Sydney (Australia), the Research Center (FZK) Karlsruhe and the University of Stuttgart (Germany). Similar submillimeter wavelength gyrotrons are also being developed at the Institute of Applied Physics in Nizhny Novgorod (Russia) [1] and at the Massachusetts Institute of Technology (USA) [2]. A quasi-optical gyrotron for plasma diagnostics is under development in cooperation with the National Institute for Fusion Science (NIFS) in Japan. It is expected that this device will achieve frequency tunability in two frequency bands, namely near 92 GHz at fundamental operation and near 184 GHz at second harmonic.

This paper summarizes the achievements of the Gyrotron FU series and presents the status of the development of the quasi-optical gyrotron.

2. Gyrotron FU series

The gyrotrons belonging to the Gyrotron FU series are frequency step-tunable sources of microwave radiation covering a wide wavelength range from the millimeter to the submillimeter region. The output power of these devices is not so high, ranging from several hundred watt to several ten kilowatt for fundamental operation and from several ten watt to several kilowatts for second harmonic operation. The main results are summarized as follows:

2.1. Frequency tunability in broad band from 38 to 889 GHz [3–5]

All frequencies achieved up to now by 5 gyrotrons included in the Gyrotron FU series are summarized as a function of the field intensity B_0 in Fig. 1. The solid lines represent the fundamental ($f = f_c$), the second ($f = 2f_c$) and the third ($f = 3f_c$) harmonic resonances. Frequency step-tunability from 38 to 889 GHz bas been achieved operating the gyrotrons at the fundamental, second and third harmonics of the cyclotron frequency. The gyrotron FU IVA has achieved the highest frequency, namely 889 GHz for single-mode operation on the $TE_{8,6,1}$ cavity mode at the second harmonic ($f = 2f_c$). The corresponding wavelength is 337 μm.

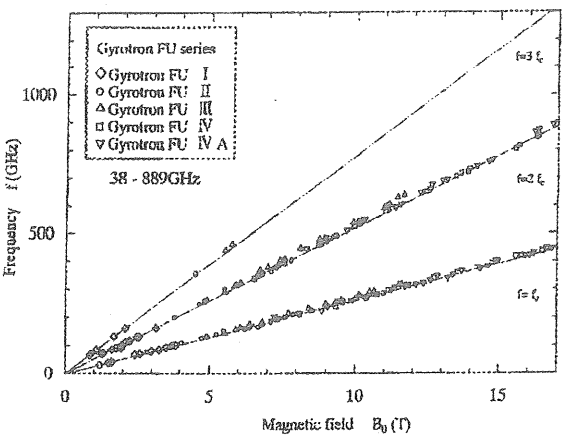

Fig. 1. All frequencies achieved up to the present by the Gyrotron FU series as a function of field intensity B_0. Solid curves show the fundamental, the second and the third harmonic resonances.

2.2. Amplitude modulation [6,7]

The gyrotrons FU III and FU IV have achieved amplitude modulation of their output radiation. The mechanism of amplitude modulation is based on the strong dependence of the efficiency of interaction between the electron beam and the microwave field in the cavity on the velocity distribution of the electrons. The velocity distribution function and, in particular, the average pitch factor of the beam can be varied by changing the anode potential. Therefore, modulation of the anode voltage V_a leads to modulation of the gyrotron output. Fig. 2 shows a typical result of amplitude modulation in the submillimeter wavelength gyrotron FU III with the ratio $\Delta V_a/V_a$ (modulation level) as

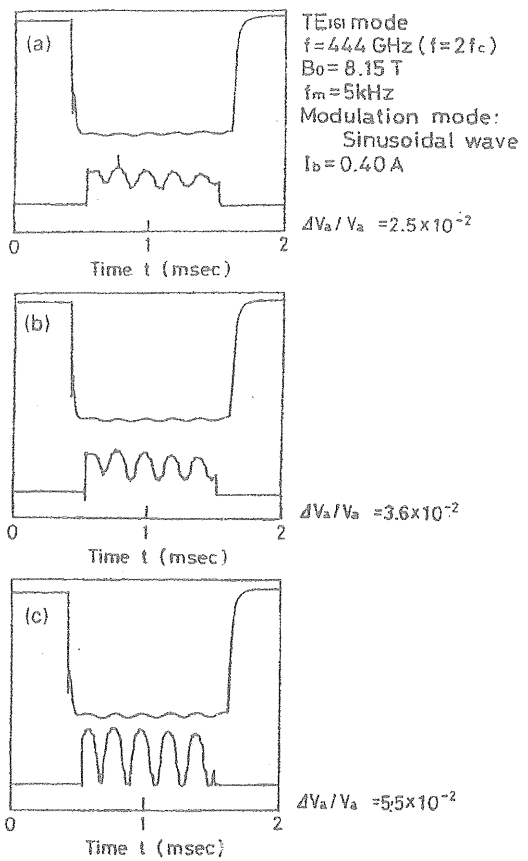

Fig. 2. Amplitude modulation result for Gyrotron FU III. Upper traces are high-voltage pulses applied to the anode and lower traces are output powers of the gyrotron. Unmodulated beam voltage is $V_b = 40$ kV, other parameters are shown in the figure.

a parameter. In this case, the gyrotron was operated on the second harmonics of the cyclotron frequency. The cavity mode is $TE_{1,6,1}$, the frequency is 444 GHz, and the output power is about 300 W. The upper traces of Fig. 2 show the high-voltage pulse applied to the anode. Also seen on these traces is the small sinusoidal modulation of this pulse. The lower traces show the output power of the gyrotron. The modulation rate $\Delta P_{out}/P_{out}$ of the gyrotron output increases with the modulation rate $\Delta V_a/V_a$ of the anode voltage. A modulation of 100% ($\Delta P_{out}/P_{out} = 1$) is attained when $\Delta V_a/V_a$ is only several percent ($\Delta V_a/V_a \approx 0.055$). It is important to notice that the modulation rate $\Delta P_{out}/P_{out}$ is almost linearly proportional to $\Delta V_a/V_a$. This means

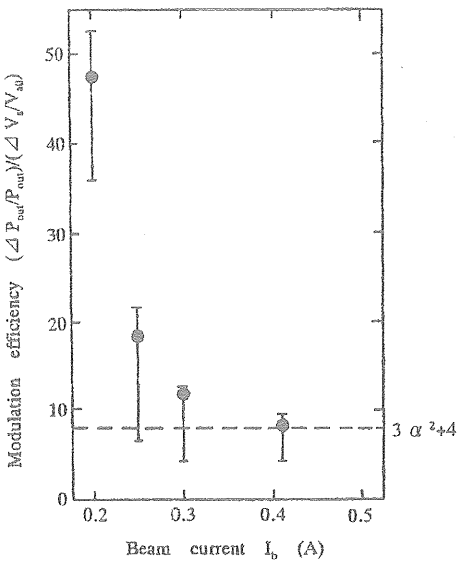

Fig. 3. Amplitude modulation efficiency $(\Delta P_{out}/P_{out})/(\Delta V_a/V_a)$ as a function of the beam current I_b.

that sinusoidal modulation of the output power is possible using sinusoidal modulation of the anode potential. Such sinusoidal modulation at frequencies up to 600 kHz has been achieved at low values of $\Delta V_a/V_a \sim 1.1 \times 10^{-3}$. The efficiency of the amplitude modulation $(\Delta P_{out}/P_{out})/(\Delta V_a/V_a)$ is plotted as a function of the beam current I_b in Fig. 3. The theoretical prediction for the efficiency is derived from the energy transfer between the electrons and the electromagnetic wave in the following form:

$$(\Delta P_{out}/P_{out})/(\Delta V_a/V_a) = (1 + P_{ohm}/P_{out})(3\alpha^2 + 4), \quad (1)$$

where P_{ohm} is the ohmic power loss in the cavity and α is the pitch angle of beam electrons. The broken line in Fig. 3 shows the efficiency when the term P_{ohm}/P_{out} is not taken into account. It can be seen in this figure that the experimentally obtained efficiency is closer to the theoretical prediction (broken line) for big values of I_b (corresponding to big values of P_{out}) when the term P_{ohm}/P_{out} can be neglected.

2.3. Frequency modulation [8]

The gyrotron FU IV has achieved frequency modulation within the limits of the resonance

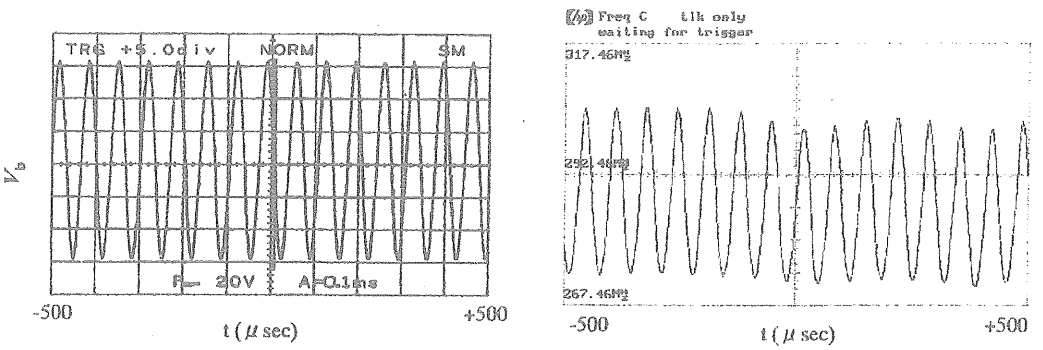

Fig. 4. Typical experimental results of frequency modulation. The traces show the modulation of V_b (on the left-hand side) and the modulation of the output frequency which is represented by modulation of f_{IF} (ons the right-hand side); f_m = 156 kHz, ΔV_b = 120 V and Δf = 31.1 MHz.

frequency linewidth of the cavity mode. The principle of the frequency modulation is based on the dependence of the cyclotron frequency on the relativistic mass factor. Thus, modulation of the energy of the beam electrons results in modulation of the frequency of generated radiation. In our experiments for this purpose, the body potential (which determines the accelerating voltage and hence the energy of electrons) has been modulated. The body of the tube includes the cavity and is separated electrically from the beam collector by a ceramic insulator. The output power is transmitted by circular wave guides and is emitted to a horn antenna. The frequency is measured by heterodyne detection system consisting of a sweep oscillator, a frequency counter, a harmonic mixer and a modulation domain analyzer. The detected signal (f) is mixed with a high harmonic of the local oscillator and converted to a low-frequency signal (f_{IF}). The time and frequency resolutions of the detection system used are 10 μs and 10 kHz, respectively.

A typical result of the frequency modulation experiment is presented in Fig. 4. The trace on the left-hand side shows the sinusoidal modulation of the body potential V_b. The amplitude of the modulation is around 120 V. The corresponding frequency modulation can be seen in the f_{IF} trace on the right-hand side. It is also close to sinusoidal modulation and the amplitude is about 30 MHz. In this example, the modulation frequency f_m is 10 kHz.

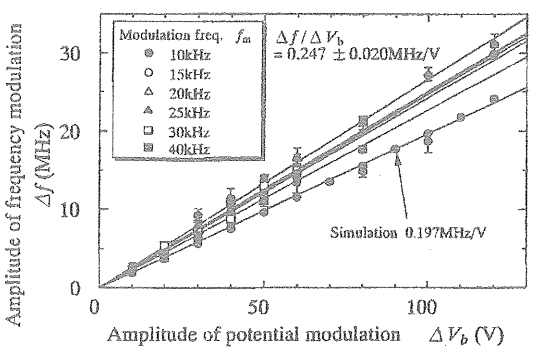

Fig. 5. Experimental and simulation results for frequency modulation amplitude Δf versus the amplitude of the body potential modulation ΔV_b for f_m = 10, 15, 20, 25, 30 and 40 kHz. Observed frequency modulation efficiency $\Delta f/\Delta V_b$ = 0.247 MHz/V, output power P = 20 W.

The amplitude of frequency modulation Δf versus the amplitude of the body potential modulation ΔV_b is plotted in Fig. 5 for several values of modulation frequency f_m. The efficiency of frequency modulation is MHz/V. The results of simulations are also indicated by solid circles. The estimated efficiency $\Delta f/\Delta V_b$ = 0.247is distributed close to the experimentally obtained values. This submillimeter wavelength gyrotron is used as a radiation source for plasma scattering measurements and ESR experiments in our laboratory. For these applications, modulation of both the output power and frequency is very useful.

2.4. Complete cw operation with high stability of amplitude and frequency

One of the advantages of the complete cw operation is the stabilization of the frequency and the amplitude of the gyrotron output. The longest period of operation was 15 h. This means "complete cw" regime. In our experiments we use a current-stabilized high-voltage power supply in order to ensure stable operation. The variations of the output frequency were measured by a time-resolved system which is basically the same as the system used for measurement of the frequency modulation. The measured frequency variations δf during 100 ms are several MHz and $\delta f/f$ is of the order of 10^{-5} for several cavity modes. The output power variations measured by Schottky diode during 10 min are several percent. These variations are the result of small fluctuations of the anode and cathode voltages of the electron gun. We are planning to stabilize both the voltages and then to realize a feed-back control, in such a way further high quality stabilization will be achieved. Fig. 6 shows a preliminary result of amplitude stabilization by feed-back control of the anode voltage. It can be seen in the upper trace that the fluctuation level of the amplitude is decreased significantly. An estimate, based on the experimental measurements, indicates that the fluctuations are less than 0.1%.

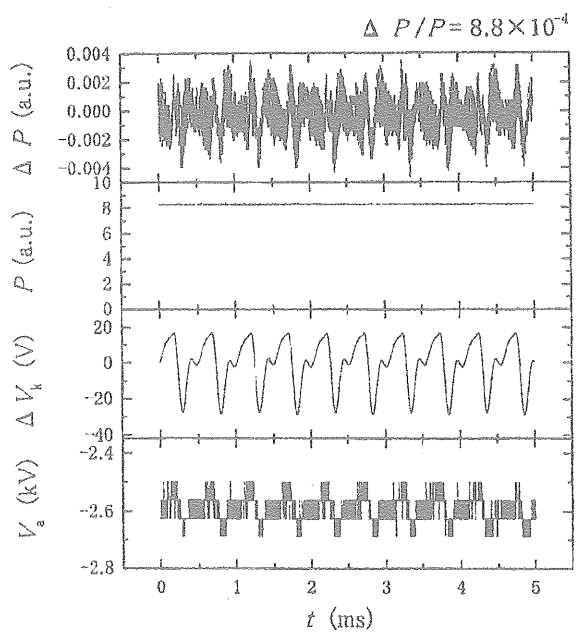

Fig. 6. A typical result of amplitude stabilization experiment by feed-back control of the anode voltage V_a. The traces represent (from top to bottom): fluctuation of the output power, output power, variation of the cathode voltage and anode potential.

3. Quasi-optical gyrotron

A schematic drawing of the quasi-optical gyrotron which is being developed in a collaboration between NIFS and Fukui University is shown in Fig. 7. In this gyrotron, a Fabry–Perot resonator is installed. It enables frequency tuning in wide ranges near 90 and 180 GHz. The tunability is around 20%. The operational parameters of the gyrotron are listed in Table 1. The output power, estimated from computer simulation, is about 100 kW for fundamental and 50 kW for the second harmonic operation. Frequency tunability of such a high-power gyrotron will be useful for a variety of applications, for example, plasma diagnostics and high-power spectroscopy. The quasi-optical gyrotron will be installed on the large helical device (LHD) in NIFS and will be used for Thomson scattering measurements of ion temperature.

Table 1
Operational parameters of the quasi-optical gyrotron

Frequency range	80–100 GHz (fundamental operation) 160–200 GHz (second harmonic operation)
Output power	~ 100 kW (fundamental operation) ~ 50 kW (second harmonic operation)
Efficiency	20–30% (fundamental operation) 10–20% (second harmonic operation)
Maximum field intensity	4.5 T
Parameters of the electron beam	70 kV, 10 A, 1 ms (first stage) 80 kV, 20 A, 10 ms (final stage)

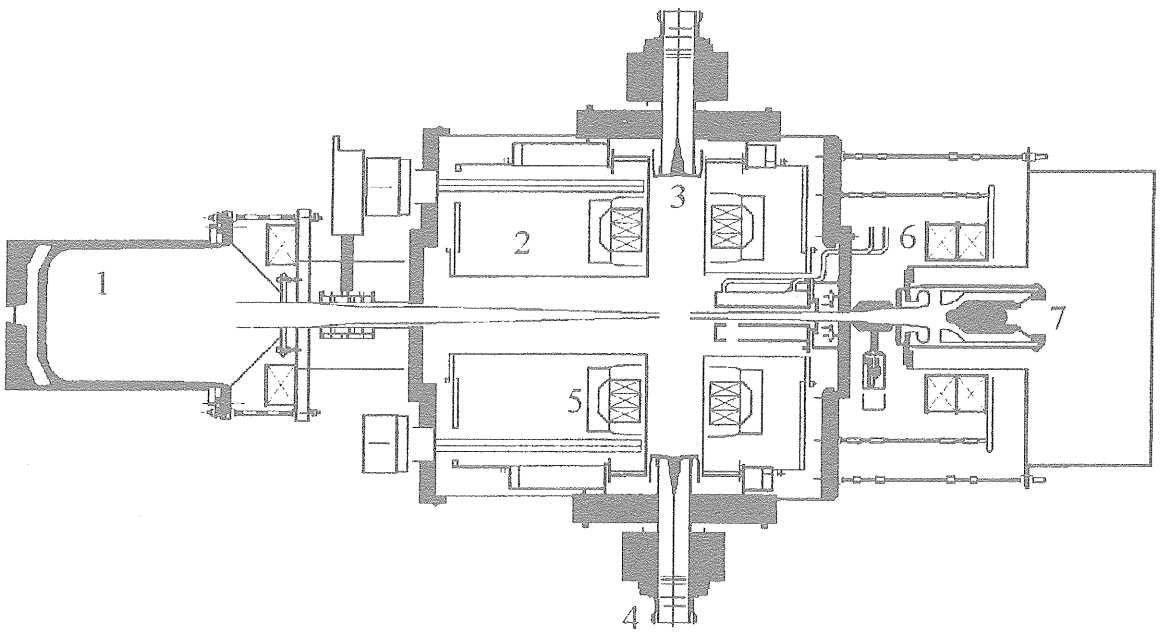

Fig. 7. A schematic drawing of the quasi-optical gyrotron (1 — collector, 2 — cryostat, 3 — Fabry–Perot resonator, 4 — RF window, 5 — superconducting magnet, 6 — gun coils, 7 — magnetron injection gun).

4. Applications of Gyrotron FU series

4.1. Application to plasma scattering measurements

The Gyrotron FU II has been employed as a radiation source for plasma scattering measurements on the compact helical system (CHS) at NIFS. The gyrotrons are well suited for such measurements due to their capability to radiate powerful microwaves in the submillimeter wavelength range. For example, the gyrotron FU II delivers long pulses (varied up to 0.6 s) of moderately high power (~ 110 W) at submillimeter wavelengths ($\lambda = 0.847$ mm, $f \sim 345$ GHz) [9]. Utilization of such gyrotrons enables one to improve the S/N ratio of the measurements and to observe low-level density fluctuations.

Fig. 8 shows the installation used for scattering experiments on CHS. The gyrotron output is converted to a linearly polarized, quasi-Gaussian beam and transmitted by a quasi-optical mirror system before it is injected into the plasma. The wave scattered from the plasma is received by a horn antenna installed in the plasma vessel. It is converted into a low-frequency signal by a homodyne detection system. The measurements at scattering angles of 4.4 and 8.8° are carried out in neutral beam injection (NBI)-heated plasma and in ion cyclotron resonance frequency (ICRF)-heated plasmas. A typical result of scattering measurement at

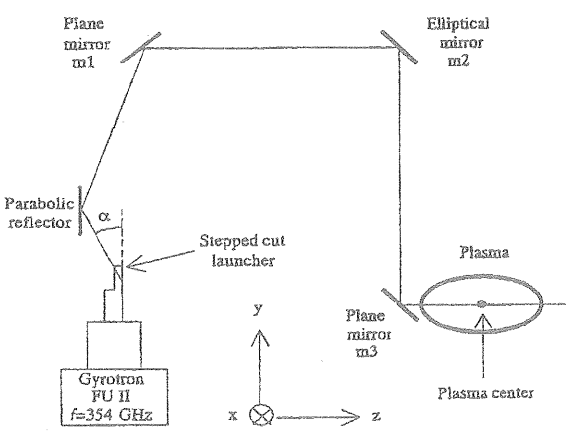

Fig. 8. A schematic drawing of the installation for scattering measurements using Gyrotron FU II on CHS.

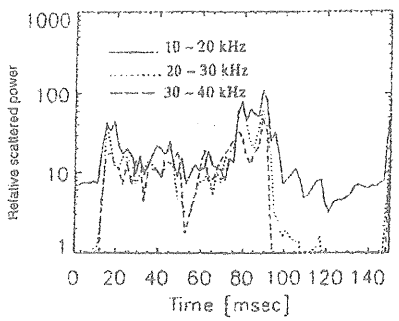

Fig. 9. Time evolution of the scattered wave power relative to the power scattered prior to the ICRF heating pulse (the traces correspond to the frequency intervals 10–20, 20–30 and 30–40 kHz, respectively).

an angle of 8.8° for NBI-heated plasma suggests an excitation of a drift wave. The plasma was produced by a microwave pulse for electron cyclotron heating (ECH) and heated by a NBI pulse. In this experiment, frequency spectra of the scattered signals have been registered. Each spectrum covers frequency band from 0 to 1 MHz and has been obtained in a 20 ms time period. Some broadening of the spectrum during NBI heating has been observed. After the NBI pulse, such broadening has not been detected. The broadening up to about 600 kHz is possibly due to scattering by drift waves excited spontaneously in the NBI heating phase.

Fig. 9 shows a result of scattering measurement for ICRF-heated plasma. The plasma is initiated at the time of 10 ms on the horizontal axis by an ECH pulse. An ICRF heating pulse is then applied in the time interval from 40 to 90 ms. The traces show the time evolution of the scattered wave power relative to the power scattered prior to the ICRF heating pulse. Each curve stands for one of the frequency intervals: 10–20, 20–30 and 30–40 kHz, respectively. The scattering angle of 8.8° corresponds to a wave number of $11.4\,cm^{-1}$. The increase in scattered wave power is observed during the ICRF heating. Reflection measurement using a reflectometer was performed at the same time. The results are in reasonable agreement with the scattering measurement and support the applicability of both techniques.

Observed scattered signals suggest that some instability related with the drift wave occurs during NBI or ICRF heating. This phenomenon would have an adverse effect on the plasma confinement. We plan to continue the measurements on CHS and LHD under various plasma parameters in order to study the effect of this instability on the plasma confinement.

4.2. Application to ESR experiments [10,11]

The gyrotrons FU I, FU E, FU IV and FU IVA are being employed as radiation sources for ESR spectroscopy. In this field, the millimeter and submillimeter gyrotrons have several clear advantages over the other conventional sources. For example, they offer frequency tunability in broad bands and relatively high-output power. Due to such favorable features our gyrotrons are suitable for ESR studies and especially for investigation of nonlinear ESR phenomena.

A block diagram of an ESR spectrometer in which the gyrotron FU I is embedded as a radiation source is presented in Fig. 10. The spectrometer includes a pulse magnet which produces strong magnetic fields up to 30 T. The output power of the gyrotron is transmitted to the sample through an oversized circular wave guide. The transmitted power is detected by a crystal detector or an InSb electron detector.

An ESR spectrum of Cr^{3+} in dark ruby was registered using the gyrotron FU IV as a radiation power source. Fig. 11 shows a typical result obtained by sweeping the magnetic field. The parameter in these plots is the observed frequency ν. Absorption signals are registered at three different magnetic fields corresponding to fine structure transitions of the spin state interval A^4 — ground state of Cr^{3+}. An ESR signal of a DPPH standard reference sample is shown on each trace as an indicative marker of the magnetic field. It should be noted that the resonant magnetic field depends on the orientation of the c-axis. The spectrum presented in Fig. 11 corresponds to a magnetic field perpendicular to the c-axis of ruby.

The field intensities H_0 corresponding to the resonant absorption are plotted in Fig. 12 as a function of the angle θ between the direction of the magnetic field and the c-axis of ruby. The solid curves represent results of calculations. The g-factors

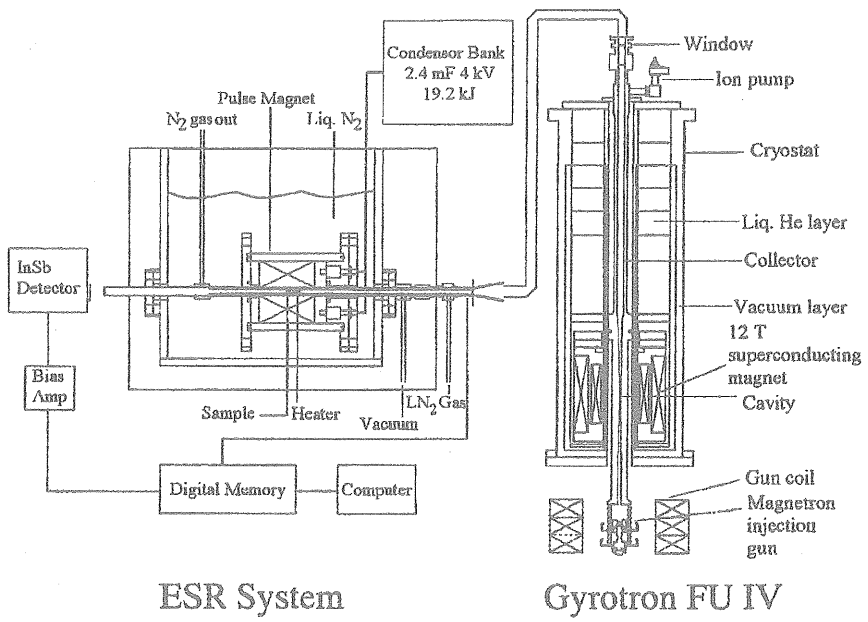

Fig. 10. A block diagram of ESR spectrometer using Gyrotron FU IV as a radiation source.

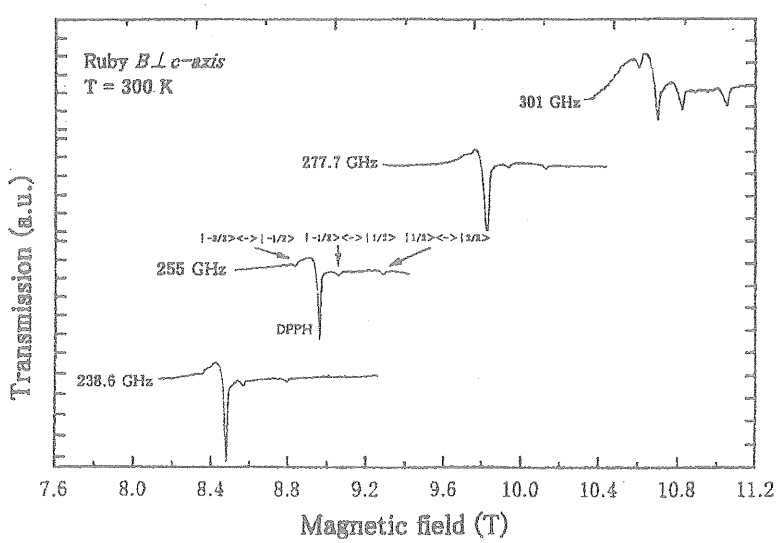

Fig. 11. ESR spectrum of Cr^{3+} (A^4) in ruby as a function of magnetic field H_0 and observed frequency ν as a parameter. On each trace, ESR signal from DPPH is seen as an indicative marker for the intensity of the magnetic field.

and the fine structure constant D which fit the experimental results best are

$$g_{\parallel} = 1.9803, g_{\perp} = 1.9813 \text{ and } D = -5.742\,\text{GHz}.$$

Fig. 13 presents the dependency of the fine structure constants on the frequency. The solid curve is calculated using a formula which includes ν^2 terms. It seems that the experimental results are in good

agreement with the calculations. Such ESR studies at higher frequencies give more insights in understanding the variations of D. A further extension of the ESR experiments to a broader frequency band is in progress now.

5. Summary

We have developed frequency-tunable, medium-power, submillimeter wavelength gyrotrons (Gyrotron FU series) and a high-power quasi-optical millimeter wavelength gyrotron. These devices

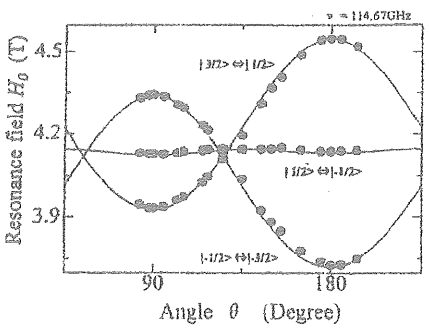

Fig. 12. Angular dependence of three ESR transition lines of Cr^{3+} (A^4)in ruby. Solid lines are results calculated taking into account third-order perturbation of the Price Hamiltonian.

are suitable radiation sources for a wide variety of applications including plasma diagnostics and millimeter to submillimeter wavelength spectroscopy.

At present, the Gyrotron FU series in Fukui University consists of eight gyrotrons. Each of them is designed to operate on many single modes at fundamental, second and even third harmonics of the electron cyclotron resonance. Such design determines their most distinguishing features which allow one to classify them as high-frequency, medium-power gyrotrons covering a broad frequency band from millimeter-to-submillimeter wavelength region. The main results achieved by our gyrotrons are summarized as follows:

(1) These gyrotrons have achieved frequency tunability from 38 to 889 GHz.

(2) The amplitude and frequency modulation achieved by the gyrotrons broadens significantly their applicability to different new fields of basic research and technology.

(3) Complete cw operation has been performed with high stability of the amplitude and frequency of the gyrotron output. The level of the fluctuations of the output power has been decreased considerably and it is now less than 0.1%.

These advantages of the gyrotron series have enabled us to apply our gyrotrons to high-power, millimeter-to-submillimeter wavelength spectro-

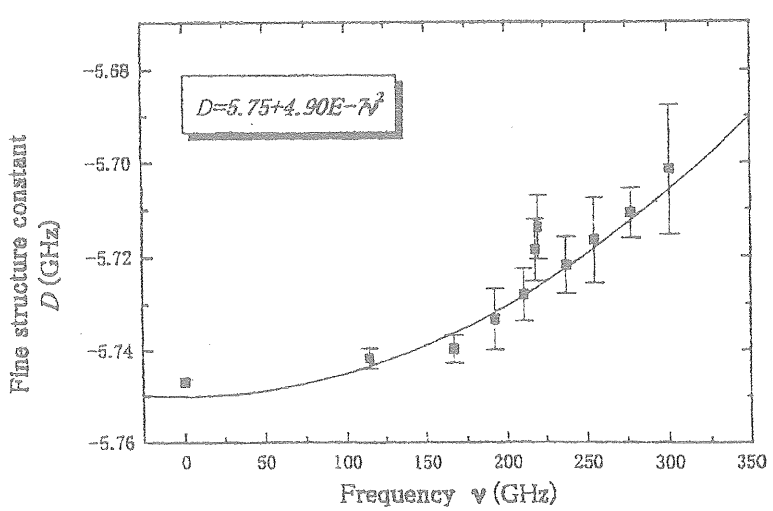

Fig. 13. The fine structure constant D of Cr^{3+} (A^4)in ruby versus the resonance frequency. Solid lines are calculation results indicating that D is proportional to ν^2.

scopy. The gyrotron FU II has already been employed for plasma scattering measurements on CHS at NIFS. The gyrotrons FU I, FU E and FU IVA have been used in ESR experiments to study frequency dependency of the fine structure constant D of ruby. The quasi-optical gyrotron will be used for measurement on LHD in NIFS in the near future.

The newest member of the FU series, gyrotron FU V, has just been constructed and has begun to operate. It has a helium-free 8 T superconducting magnet and a demountable tube. It is expected that this device will achieve time-unlimited, high-quality mode operation and will be used for far-infrared spectroscopy.

Acknowledgements

The authors wish to express their sincere thanks to Professor M. Thumm from the Research Center (FZK) Karlsruhe, Dr. W. Kasparek from the University of Stuttgart and Dr. G.F. Brand from the University of Sydney for their continuing cooperation. The work was supported by Grant-in-Aids for Scientific Research from the Ministry of Education, Science and Culture.

References

[1] Andronov AA, Flyagin VA, Gaponov VA, Goldenberg AL, Petelin MI, Usov VG, Yulpatov VK. Infrared Phys 1978;18:385.
[2] Spira-Hakkarainen SE, Kreischer KE, Temkin RJ. IEEE Trans. Plasma Sci 1990:18:334.
[3] Idehara T, Nishida N, Yoshida K, Ogawa I, Tatsukawa T,Wagner, Gantenbein D, Kasparek G, Thumm W. Int J Infrared Millimeter Waves 1998;19:919.
[4] Idehara T, Shimizu Y, Ichikawa K, Makino S, Shibutani K, Tatsukawa T, Ogawa I, Okazaki Y, Okamoto T. Phys Plasmas 1995;2:3246.
[5] Shimizu Y, Makino S, Ichikawa K, Kanemaki T, Ogawa I, Tatsukawa T, Idehara T. Phys Plasmas 1995:2:2110.
[6] Idehara T, Shimizu Y, Makino S, Ichikawa K, Tatsukawa T, Ogawa I, Brand GF. Phys Plasmas 1994;1:461.
[7] Idehara T, Shimizu Y, Makino S, Ichikawa K, Tatsukawa T, Ogawa I, Brand GF. Int J Infrared Millimeter Waves 1997;18:391.
[8] Idehara T, Pereyaslavets M, Nishida N, Yoshida K, Ogawa I. Phys Rev Lett 1998;81:1973.
[9] Ogawa I, Yoshisue K, Ibe H, Idehara T, Kawahata K. Rev Sci Instrum 1994;65:1788.
[10] Tatsukawa T, Maeda T, Sasai H, Idehara T, Mekata M, Saito T, Kanemaki T. Int J Infrared Millimeter Waves 1995;16:293.
[11] Tatsukawa T, Shirai T, Imaizumi t, Idehara T, Ogawa I, Kanemaki T. Int J Infrared Millimeter Waves 1998;19:859.